Investigation of infrared transmittivity of Y_2O_3/diamond films

Rongfa Chen (陈荣发)[1*], Zhaoxia Shen (沈兆侠)[1], Lianggang Dai (戴良刚)[1], Xianliang Zhang (张显亮)[1], Rui Zhu (朱 瑞)[1], and Dunwen Zuo (左敦稳)[2]

[1]*Department of Mechanical Engineering, Yangzhou University, Yangzhou 225009, China*

[2]*Department of Mechanical and Electrical Engineering, Nanjing University of Aeronautics and Astronautics, Nanjingare 210016, China*

[*]*E-mail: rfchen@yzu.edu.cn*

Received December 8, 2009

Optical grade thick diamond films are polished on two sides by electron discharge machining (EDM) are with a mechanical method. The infrared transmittivities of Y_2O_3/diamond films are investigated in detail. Results indicate that the average infrared transmittivity is improved from 68.82% to 82.42% after deposition of Y_2O_3 at 10-μm central wavelength, and from 67.98% to 82.45% at 8–12-μm wave-band. The coated films meet the demands of infrared window applications. Therefore, the performance of the optical-class diamond thick films used in an actual infrared window can provide reliable application for basic research.

OCIS codes: 160.4760, 240.0310, 240.6700, 310.6860.

doi: 10.3788/COL201008S1.0130.

Optical-class thick diamond films have shown excellent performance in infrared transmission of windows. Infrared transmission is mainly related to the surface integrity and intrinsic quality[1−6]. The polished surface has been investigated from different angles. Results are found to be beneficial to the study of infrared transmittance[7−12].

In this letter, scanning electron microscope (SEM) and atomic force microscope (AFM) are used to evaluate the surface morphology of the Y_2O_3/diamond films. Also, X-ray diffraction (XRD) is used to investigate the purity of Y_2O_3 coating. The infrared transmittivity of Y_2O_3/diamond films is measured by Varian FT-IR 7000 Stingray imaging system (USA). The performance provides reliable application of basic research for optical-class thick diamond films when used in actual infrared windows[13,14].

A 30-kW high power digital camera (DC) arc plasma jet chemical vapor deposition (CVD) system equipped with magnetic field was used for the experiment. The double-sided polishing was carried out by electron discharge machining (EDM) and mechanical polishing technology. The double-sided polished diamond was ultrasonically cleaned by acetone for 30 min and dried in a vacuum chamber for 10 min. Y_2O_3 coating was prepared by electron beam evaporation on the surface of the diamond substrate. The coating equipment was a BAK760 (Switzerland). Film thickness was measured by a quartz crystal film thickness monitor during coating. Y_2O_3/diamond films were characterized by SEM, AFM, and XRD spectra. Varian FT-IR 7000 Stingray imaging system was used to measure infrared transmittance.

When a cluster of infrared light with relative radiation produce incident waves upon the thick diamond film, interface (1) (normally, nucleation surface) is achieved and reaches interface (2). Then, infrared transmittance of the diamond thick film becomes $\tau(\lambda)$, which can be written as

$$\tau_\lambda = \tau_1(\lambda) \cdot \tau_2(\lambda) \cdot \tau_i(\lambda), \quad (1)$$

where $\tau(\lambda)$ is equivalent to the two surface transmission rate $\tau_1(\lambda)$ and $\tau_2(\lambda)$, while $\tau_i(\lambda)$ is internal transmittance, $i = 1,2$, as shown in Fig. 1.

The transmission of radiated power $\Phi_{\lambda x}$ along the distance from surface (1) to (2) of the thick diamond film can be written as

$$\Phi_{\lambda x}(x) = \Phi_{\lambda x}(0) \exp\{[-\alpha(x)n_a + \gamma'(\lambda)n_a]x\}, \quad (2)$$

where $\gamma'(\lambda)$ is scattering coefficient, $\Phi_{\lambda x}$ is incident power, $\alpha'(\lambda)$ is absorption coefficient of the grain concentration, and n_γ is concentration of grain. It decreases when the concentration of absorbing and scattering grain increases.

From Eqs. (1) and (2), we can see that the transmittance of the thick diamond film $\tau(\lambda)$ is the equivalent of two interface transmission rate $\tau_1(\lambda)$ and $\tau_2(\lambda)$, and internal transmittance, $\tau_i(\lambda)$. Herein, $\tau_1(\lambda)$ and $\tau_2(\lambda)$ are connected by two surface morphology and surface roughness, while $\tau_i(\lambda)$ is closely related with internal stress, grain size, and concentration. This study is of great significance when one aims to understand the mechanism of infrared waves through a diamond window.

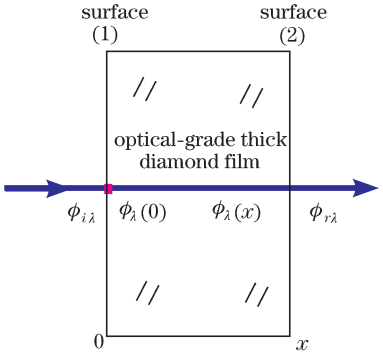

Fig. 1. Schematic of infrared light waves through the thick diamond film.

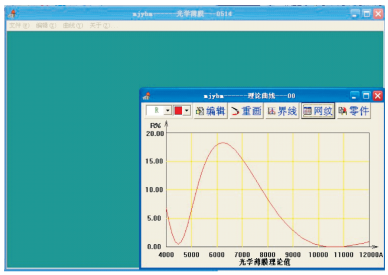

Fig. 2. Main window of simulation software of antireflection coating.

Fig. 3. Window of input parameter.

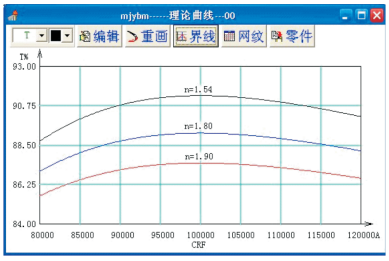

Fig. 4. Transmittance curve of antireflection coating.

On the bases of thin film composite (TFC) and Essential Macleod, Delphi was used as basic controls. The main window of the infrared simulation calculation of transmittance is shown in Fig. 2. Various parameters are entered through the window, as shown in Fig. 3. After iterative calculation, the infrared transmittance curve of antireflection coating can be obtained, as shown in Fig. 4. From the simulated results, the transmission rate of Y_2O_3 coating is given as 89.28% at the center wavelength of 10 μm.

The surface of Y_2O_3 coating prepared by electron beam evaporation is shown in Fig. 5. The average diameter of the grains is 28.6 nm. Y_2O_3 coating is smooth and bright in color; the surface integrity is very good and without any holes or accumulation of defects. The cross-sectional structure of Y_2O_3/diamond films is shown in Fig. 6. Film density is better and film thickness dispersion is smaller. Similarly, voids do not appear at the coating, no particle impurities can be observed, and the coating thickness of Y_2O_3 is uniform. The XRD spectrum of the Y_2O_3 coating is shown in Fig. 7. The characteristic peaks of diamond (111) and (220) are significant, although the peak intensity of (111) is higher than that of (220). Meanwhile, the characteristic peaks of Y_2O_3 coating (111) and (400) also achieve the certain peak strength, with the peak intensity of (400) higher than

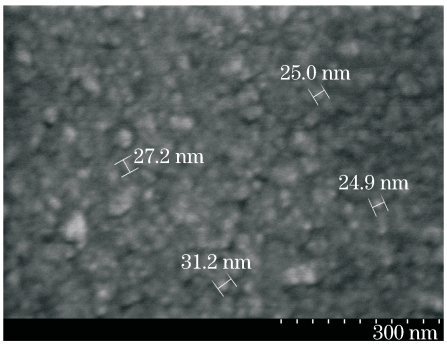

Fig. 5. SEM of Y_2O_3 coating.

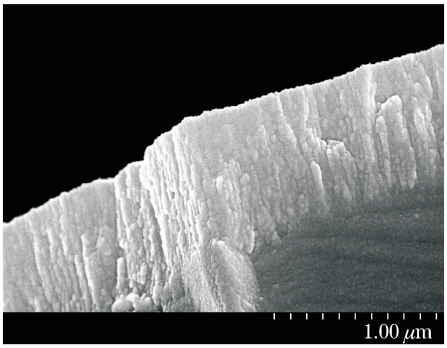

Fig. 6. SEM of the cross-section structure of Y_2O_3 coating.

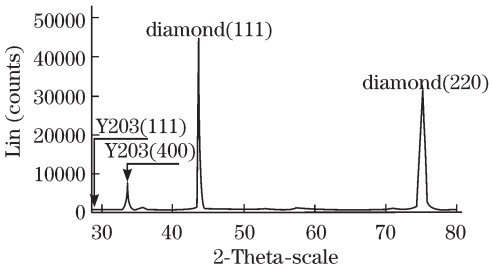

Fig. 7. XRD spectrum of the Y_2O_3 coating.

that of (111). There is no other impurity peak intensity, thus indicating that the diamond substrate and Y_2O_3 coating is of high purity. The results meet the requirements of infrared transmittance.

With infrared transmission rate in the center wavelength of 10 μm at 68.82%, the average transmission rate is 67.98% at 8−12 μm before the coating deposition. Infrared transmittance curve after deposition of Y_2O_3 coating is shown in Fig. 8. It can be seen that transmission rate is 82.42% at the center wavelength of 10 μm, or an increase of 13.60%. Average infrared transmission rate is 82.45% at the 8−12 μm band, or an increase of 14.47%, as shown in Fig. 9. The measured transmission rate is lower than the theoretical 89.28% at the central wavelength of 10 μm. The main reasons for these are the growth process of the diamond, the large columnar grain structure, and a variety of surface defects, which can lead to much scattering and absorption. Figure 10 shows the AFM of defects of Y_2O_3 coating on the growth surface of diamond, although surface roughness is very small (Ra is only 12.72 nm).

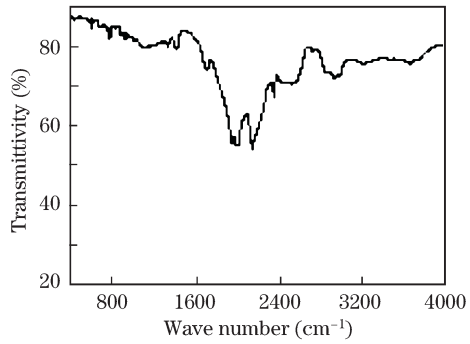

Fig. 8. Transmittance curve of Y_2O_3 coating.

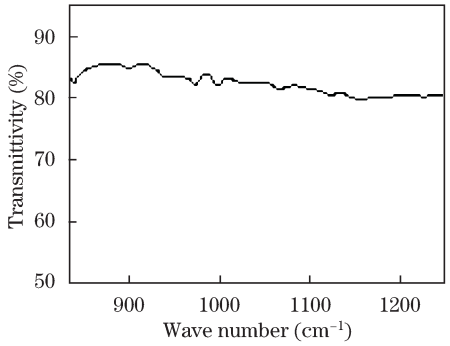

Fig. 9. Transmittance curve at 8−12 μm.

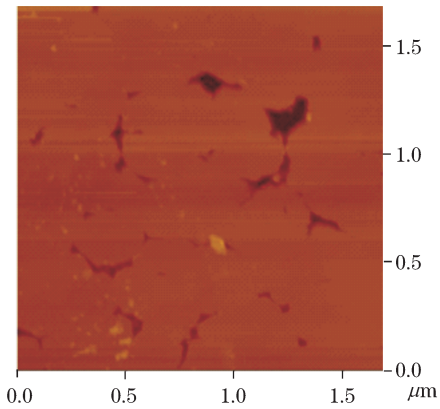

(a) Surface morphology of AFM

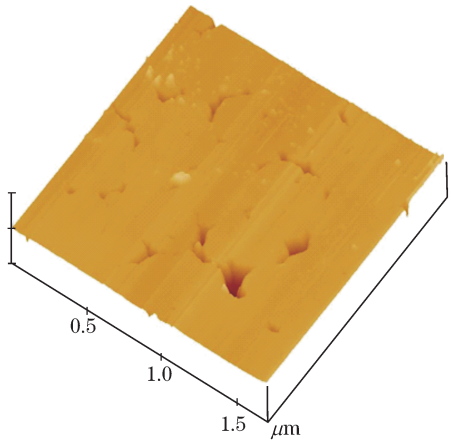

(b) Surface morphology in 3D

Fig. 10. AFM of defects of Y_2O_3 coating on growth surface of diamond.

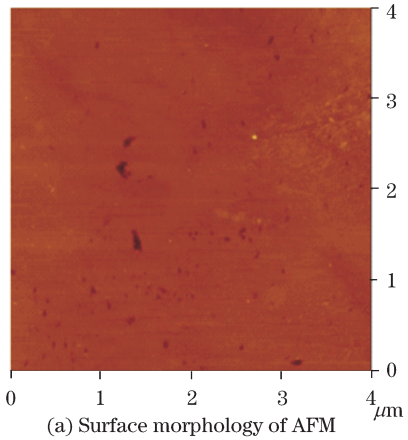

(a) Surface morphology of AFM

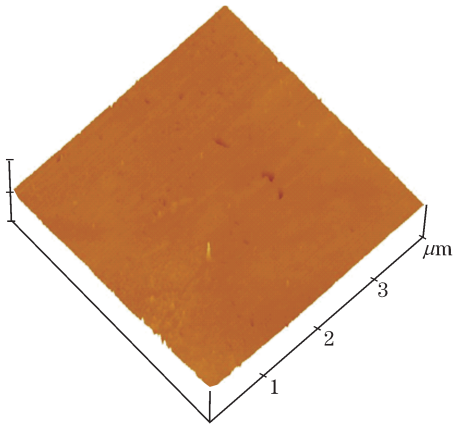

(b) Surface morphology in 3D

Fig. 11. AFM of defects of Y_2O_3 coating on nucleation surface of diamond.

Similarly, growth defects (i.e., holes, steps, dislocations and relaxation, among others) still cannot be eliminated after polishing. AFM analysis of the nucleation surface is shown in Fig. 11. Ra is 11.12 nm, and the micro-structural defects are observed to be caused by the growth competition process. Infrared transmission rate $\tau(\lambda)$ has toned down to about 6.86% by the surface defects at center wavelength of 10 μm.

Optical thin film software Macleod and TFC are used to simulate refractive index of Y_2O_3 antireflective coating against antireflection. The transmission rate of Y_2O_3 coating is 89.28% at the center wavelength of 10 μm. Y_2O_3 coating is deposited with electron beam evaporation at a high vacuum environment. The film density is better and film thickness dispersion is smaller upon SEM observation. Y_2O_3 coating is of high purity based on XRD analysis. The infrared transmittivity of Y_2O_3/diamond films is investigated in detail. Results indicate that the average infrared transmittivity is improved from 68.82% to 82.42% after deposition of Y_2O_3 at 10 μm central wavelength, and from 67.98% to 82.45% at 8−12 μm waveband. The coated films can meet the demands of infrared window application.

This work was supported by the Scientific Innovation Fund of Yangzhou University and the National Natural Science Foundation of China (No. 50275076).

References

1. S. W. Reeve and W. A. Weimer, Thin Solid Films **236,** 91 (1993).
2. D. Friedericke, B. Volker, P. Jurgen, and H. Gruner, Surf. Coat. Tech. **119,** 428 (1999).
3. F. X. Lu, G. F. Zhong, and J. G. Sun, Diamond Relat. Mater. **7,** 737 (1998).
4. R. F. Chen, D. W. Zuo, Y. L. Sun, W. Z. Lu, D. S. Li, and M. Wang, Adv. Mater. Res. **24-25,** 377 (2007).
5. R. F. Chen, D. W. Zuo, D. S. Li, F. Xu, T. Ji, and M. Wang, Key Eng. Mater. **359-360,** 285 (2008).
6. F. Xu, D. Zuo, R. Chen, W. Lu, and M. Wang, Key Eng. Mate. **359-360,** 319 (2008).
7. R. F. Chen, D. W. Zuo, D. S. Li, B. M. Xiang, L. G. Zhao, and M. Wang, Acta Meta. Sinica (in Chinese) **41,** 1091 (2005).
8. D. S. Li, D. W. Zuo, R. F. Chen, B. K. Xiang, and L. G. Zhao, Key Eng. Mater. **315-316,** 385 (2006).
9. R. F. Chen, D. W. Zuo, F. Xu, D. S. Li, and M. Wang, J. Mater. Sci. Technol. **23,** 495 (2007).
10. R. F. Chen, D. W. Zuo, Y. L. Sun, W. Z. Lu, D. S. Li, and M. Wang, Adv. Mater. Res. **24-25,** 377 (2007).
11. J. T. William, E. Michael, and P. Klocek, Proc. SPIE **CR64,** 137 (1996).
12. J. T. William and D. C. Harris, Proc. SPIE **1112,** 9 (1989).
13. J. T. William, Hand. Opt. Cons. Solids **1135,** 963 (1997).
14. J. T. William and E. T. Michael, Hand. Opt. Cons. Solids **1465,** 1079 (1997).